ANALYSIS OF THE FRF'S CURVE ACCURACY OF TDOF SYSTEM USING LINEAR SWEPT-SINE EXCITATION METHOD

Oleh :

Asmara Yanto
Department of Mechanical Engineering - Faculty of Industrial Technology
Institut Teknologi Padang (ITP)
Jl. Gajah Mada Kandis Nanggalo Padang, 25143, Indonesia
E-mail: asmarayanto@gmail.com

Abstrak

Pengukuran FRF (Fungsi Respon Frekuensi) memiliki peranan yang sangat penting dalam dinamika struktur. Pengukuran ini biasanya diselenggarakan untuk memperoleh kurva FRF dari sebuah sistem yang diinvestigasi. Dari kurva FRF dapat ditentukan harga frekuensi resonansi dan rasio redaman sistem. Pada pengukuran ini, sistem umumnya dieksitasi dengan palu impak atau shaker. Pengukuran FRF dengan eksitasi shaker sering dilakukan dengan metode eksitasi linear swept-sine. Makalah ini mepaparkan suatu analisa terhadap ketelitian kurva FRF yang diperoleh dari penerapan metode ini pada sebuah Sistem 2-DK (Dua Derajat Kebebasan). Ketelitian kurva FRF ditentukan dengan mengacu kepada persentase kesalahan harga magnitudo FRF dan frekuensi resonansi Sistem 2-DK yang diperoleh terhadap harga teoritiknya. Dari analisa yang dilakukan dapat disimpulkan bahwa ketelitian kurva FRF Sistem 2-DK bergantung kepada durasi eksitasi linear swept-sine yang diterapkan. Apabila eksitasi linear swept-sine diterapkan ke Sistem 2-DK dengan durasi yang lebih lama, maka persentase kesalahan magnitudo FRF dan frekuensi resonansi Sistem 2-DK yang diperoleh lebih kecil dan mendekati harga teoritiknya.

Kata kunci: kurva FRF, eksitasi linear swept-sine, Sistem 2-DK, magnitudo FRF, frekuensi resonansi, durasi eksitasi.

INTRODUCTION

Impact hammer and shaker excitation are the most commonly used excitation techniques in FRF (Frequency Response Function) measurement (Scheffer and Girdhar, 2004; Mobley, 1999; Schwarz and Richardson, 1999; McConnell, 1995). Using shaker's excitations, generally there is much better control on the frequency ranges excited as well as the level of force applied to the tested system (Peres et.al, 2010; Cloutier et.al, 2009; Füllekrug et.al., 2008). There are various type of shaker's excitations can be used, however, linear swept-sine excitation is the most common type of excitation in FRF measurement (Yanto and Abidin, 2012(a), 2012(b); Zhuge, 2009; Peeters et.al., 2008; Climent, 2007, Göge et.al., 2007; Pauwels et.al., 2006).

Linear swept-sine excitation is a sinusoidal excitation of which excitation frequencies change linearly within time (Orlando et.al, 2008; Gloth and Sinapsis, 2004(a), 2004(b); Baoliang and Xia, 2003; Haritos, 2002). Analysis of swept time (excitation's duration) and modal parameter effects on the FRF's magnitude error of SDOF (Single Degree Of Freedom) System using linear swept-sine excitation was explained by Yanto (2013). Nevertheless, application of this linear swept-sine excitation to other system as well as TDOF (Two Degree Of Freedom) should be explained too in order accuracy level of the FRF's curve obtained by this method is known well. Here, accuracy level of the FRF's curves established refers to error percentage of the obtained FRF's magnitudes and resonant frequencies values to its theoretical values of the TDOF System.

METHODOLOGY

A TDOF System contains two mass m_1 and m_2, two stiffness k_1 and k_2, two dampers c_1 and c_2, and two excitation forces $f_1(t)$ and $f_2(t)$ as shown in Figure 1(a). Two coordinates y_1 and y_2 describe both mass relative positions to its references position.

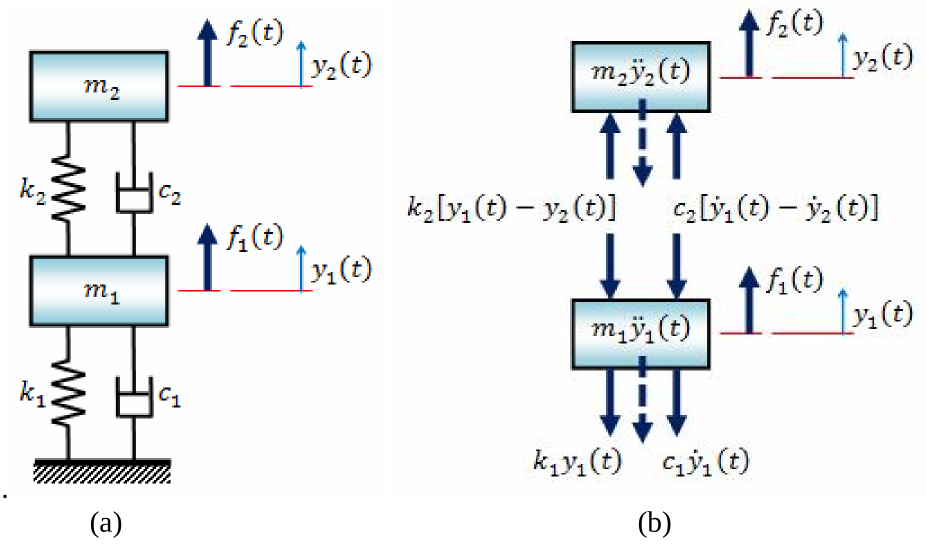

Figure 1. A TDOF System is be under excitation forces.
(a) System model (b) Free body diagram.

Free body diagram of a TDOF System model in Figure 1(a) can be illustrated by Figure 1(b). There are two free body diagrams in Figure 1(b). The first is free body diagram of m_1 and the second is free body diagram of m_2. If motion equations of a TDOF System model in Figure 1(a) are derived for each mass (see free body diagram of a TDOF System model in Figure 1(b)), then obtained

$$m_1\ddot{y}_1(t)+c_1\dot{y}_1(t)+c_2[\dot{y}_1(t)-\dot{y}_2(t)]+k_1y_1(t)+k_2[y_1(t)-y_2(t)]=f_1(t) \quad \ldots (1)$$

$$m_2\ddot{y}_2(t)-c_2[\dot{y}_1(t)-\dot{y}_2(t)]-k_2[y_1(t)-y_2(t)]=f_2(t) \quad \ldots (2)$$

In matrix form, both equations (Equation (1) and Equation (2)) can be expressed with

$$\begin{bmatrix} m_1 & 0 \\ 0 & m_2 \end{bmatrix}\begin{Bmatrix} \ddot{y}_1(t) \\ \ddot{y}_2(t) \end{Bmatrix}+\begin{bmatrix} c_1+c_2 & -c_2 \\ -c_2 & c_2 \end{bmatrix}\begin{Bmatrix} \dot{y}_1(t) \\ \dot{y}_2(t) \end{Bmatrix}+\begin{bmatrix} k_1+k_2 & -k_2 \\ -k_2 & k_2 \end{bmatrix}\begin{Bmatrix} y_1(t) \\ y_2(t) \end{Bmatrix}=\begin{Bmatrix} f_1(t) \\ f_2(t) \end{Bmatrix} \quad \ldots (3)$$

With

$$[m]=\begin{bmatrix} m_1 & 0 \\ 0 & m_2 \end{bmatrix},$$

$$[c]=\begin{bmatrix} c_1+c_2 & -c_2 \\ -c_2 & c_2 \end{bmatrix},$$

$$[k]=\begin{bmatrix} k_1+k_2 & -k_2 \\ -k_2 & k_2 \end{bmatrix},$$

$$\{\ddot{y}(t)\}=\begin{Bmatrix} \ddot{y}_1(t) \\ \ddot{y}_2(t) \end{Bmatrix},$$

$$\{\dot{y}(t)\}=\begin{Bmatrix} \dot{y}_1(t) \\ \dot{y}_2(t) \end{Bmatrix},$$

$$\{y(t)\}=\begin{Bmatrix} y_1(t) \\ y_2(t) \end{Bmatrix},$$

and $\{f(t)\}=\begin{Bmatrix} f_1(t) \\ f_2(t) \end{Bmatrix},$

Equation (3) can be written in form

$$[m]\{\ddot{y}\}+[c]\{\dot{y}\}+[k]\{y\}=\{f(t)\} \quad \ldots (4)$$

By applying Laplace transformation to Equation (4) (Ogata, 2002, 1995), obtained

$$
\begin{aligned}
&[m]\{s^2\{Y(s)\}-s\{y(0)\}-\{\dot{y}(0)\}\}+[c]\{s\{Y(s)\}-s\{y(0)\}\}+[k]\{Y(s)\}=\{F(s)\}\\
&\{y(0)\}=0 \quad \text{and} \quad \dot{y}(0)=0\\
&[[m]s^2+[c]s+[k]]\{Y(s)\}=\{F(s)\}
\end{aligned}
\qquad \ldots (5)
$$

Thus, Equation (3) by applying Laplace Transformation is

$$
\begin{aligned}
&\left[\begin{bmatrix} m_1 & 0 \\ 0 & m_2 \end{bmatrix} s^2 + \begin{bmatrix} c_1+c_2 & -c_2 \\ -c_2 & c_2 \end{bmatrix} s + \begin{bmatrix} k_1+k_2 & -k_2 \\ -k_2 & k_2 \end{bmatrix}\right] \begin{Bmatrix} Y_1(s) \\ Y_2(s) \end{Bmatrix} = \begin{Bmatrix} F_1(s) \\ F_2(s) \end{Bmatrix}\\
&\begin{bmatrix} m_1 s^2 + (c_1+c_2)s + (k_1+k_2) & -(c_2 s + k_2) \\ -(c_2 s + k_2) & m_2 s^2 + c_2 s + k_2 \end{bmatrix} \begin{Bmatrix} Y_1(s) \\ Y_2(s) \end{Bmatrix} = \begin{Bmatrix} F_1(s) \\ F_2(s) \end{Bmatrix}
\end{aligned}
\qquad \ldots (6)
$$

Rewriting Equation (6), obtained

$$
\begin{Bmatrix} Y_1(s) \\ Y_2(s) \end{Bmatrix} = \begin{bmatrix} m_1 s^2 + (c_1+c_2)s + (k_1+k_2) & -(c_2 s + k_2) \\ -(c_2 s + k_2) & m_2 s^2 + c_2 s + k_2 \end{bmatrix}^{-1} \begin{Bmatrix} F_1(s) \\ F_2(s) \end{Bmatrix} \qquad \ldots (7)
$$

To solve inverse of matrix in Equation (7), let

$$
[A] = \begin{bmatrix} m_1 s^2 + (c_1+c_2)s + (k_1+k_2) & -(c_2 s + k_2) \\ -(c_2 s + k_2) & m_2 s^2 + c_2 s + k_2 \end{bmatrix} = \begin{bmatrix} a_{11} & a_{12} \\ a_{21} & a_{22} \end{bmatrix} \qquad \ldots (8)
$$

The inverse of matrix A is given by

$$
[A]^{-1} = \frac{1}{\det[A]}[C_{jk}]^T = \frac{1}{\det[A]} \begin{bmatrix} a_{22} & -a_{12} \\ -a_{21} & a_{11} \end{bmatrix} \qquad \ldots (9)
$$

Where C_{jk} is the cofactor of a_{jk} in det[A] (Kreyszig, 2006). Determinant of [A] is

$$
\begin{aligned}
\det[A] &= [m_1 s^2 + (c_1+c_2)s + (k_1+k_2)] \cdot [m_2 s^2 + c_2 s + k_2] - [-(c_2 s + k_2)]^2\\
&= m_1 m_2 s^4 + [m_1 c_2 + m_2(c_1+c_2)]s^3 + [m_1 k_2 + c_1 c_2 + m_2(k_1+k_2)]s^2\\
&\quad + (c_1 k_2 + c_2 k_1)s + k_1 k_2
\end{aligned}
\qquad \ldots (10)
$$

Thereby, the inverse of matrix A can be determined as in Equation (11).

$$
[A]^{-1} = \frac{\begin{bmatrix} m_2 s^2 + c_2 s + k_2 & c_2 s + k_2 \\ c_2 s + k_2 & m_1 s^2 + (c_1+c_2)s + (k_1+k_2) \end{bmatrix}}{\begin{pmatrix} m_1 m_2 s^4 + [m_1 c_2 + m_2(c_1+c_2)]s^3 + [m_1 k_2 + c_1 c_2 + m_2(k_1+k_2)]s^2 \\ + (c_1 k_2 + c_2 k_1)s + k_1 k_2 \end{pmatrix}} \qquad \ldots (11)
$$

Next, consider matrix G is the inverse of matrix A.

$$
[G] = [A]^{-1} \qquad \ldots (12)
$$

The matrix G contains matrix elements $G_{11}(s)$, $G_{12}(s)$, $G_{21}(s)$, and $G_{22}(s)$. Hence, Equation (6) can be written by

$$
\begin{Bmatrix} Y_1(s) \\ Y_2(s) \end{Bmatrix} = \begin{bmatrix} G_{11}(s) & G_{12}(s) \\ G_{21}(s) & G_{22}(s) \end{bmatrix} \begin{Bmatrix} F_1(s) \\ F_2(s) \end{Bmatrix} \qquad \ldots (13)
$$

Equation (13) can be illustrated with input-output relationship of the TDOF System as shown in Figure 2.

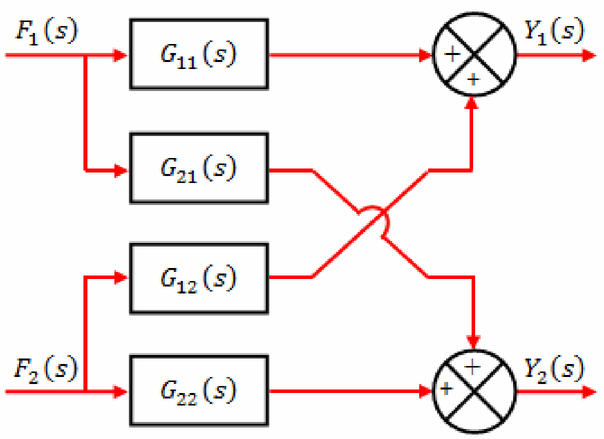

Figure 2. The input-output relationship of the TDOF System.

Furthermore, $G_{11}(s)$, $G_{12}(s)$, $G_{21}(s)$, and $G_{22}(s)$ in Figure 2 are transfer functions of the TDOF System, where subscripts are coordinate of response and stimulus respectively. The transfer functions $G_{11}(s)$, $G_{12}(s)$, $G_{21}(s)$, and $G_{22}(s)$ are expressed respectively with

$$G_{11}(s)=\frac{m_2 s^2+c_2 s+k_2}{\left(\begin{array}{c} m_1 m_2 s^4+[m_1 c_2+m_2(c_1+c_2)]s^3+[m_1 k_2+c_1 c_2+m_2(k_1+k_2)]s^2 \\ +(c_1 k_2+c_2 k_1)s+k_1 k_2 \end{array}\right)} \quad \ldots (14)$$

$$G_{12}(s)=G_{21}(s)=\frac{c_2 s+k_2}{\left(\begin{array}{c} m_1 m_2 s^4+[m_1 c_2+m_2(c_1+c_2)]s^3+[m_1 k_2+c_1 c_2+m_2(k_1+k_2)]s^2 \\ +(c_1 k_2+c_2 k_1)s+k_1 k_2 \end{array}\right)} \quad \ldots (15)$$

$$G_{22}(s)=\frac{m_1 s^2+(c_1+c_2)s+(k_1+k_2)}{\left(\begin{array}{c} m_1 m_2 s^4+[m_1 c_2+m_2(c_1+c_2)]s^3+[m_1 k_2+c_1 c_2+m_2(k_1+k_2)]s^2 \\ +(c_1 k_2+c_2 k_1)s+k_1 k_2 \end{array}\right)} \quad \ldots (16)$$

A. The theoretical FRF

The theoretical FRF of the TDOF System at certain span frequency, $H_{ij\_teo}(f)$, can be determined by evaluating system at steady state condition $(s = j\omega = j2\pi f)$.

$$H_{ij\_teo}(f)=G_{ij}(j2\pi f) \quad \ldots (17)$$

B. The FRF is obtained by the linear swept-sine excitation

The linear swept-sine excitation $u(t)$ has starting frequency f_0, ending frequency that equal to span frequency f_e, swept-time T_r, and amplitude A (Yanto, 2013). The $u(t)$ is expressed with

$$u(t)=A\sin\left(\frac{\pi}{2}(f_e-f_0)\frac{t^2}{T_r}+2\pi f_0 t\right) \quad \ldots (18)$$

The FRF of the TDOF System using the linear swept-sine excitation, $H_{ij\_lin}(f)$, is determined by

$$H_{ij\_lin}(f)=\frac{Y_i(f)}{U_j(f)} \quad \ldots (19)$$

where,

$Y_i(f) = \mathcal{F}[y(t)]$ and $U_j(f) = \mathcal{F}[u(t)]$. The $\mathcal{F}$ symbol is Fourier transformation. Subscript i is coordinate of response and subscript j is coordinate of stimulus.

RESULTS AND DISCUSSION

Value of input parameters in analysis of accuracy of the FRF's curves of the TDOF System that obtained by using the linear swept-sine excitation are shown in Table 1.

Table 1. Value of input parameters.

Parameter	Value	Unit
The TDOF System		
m_1	40	kg
m_2	10	kg
c_1	48	Ns/m
c_2	8	Ns/m
k_1	80000	N/m
k_2	40000	N/m
The linear swept-sine excitation		
f_0	0	Hz
f_e	40	Hz
A	10	N
T_r	4, 8, and 16	S

The FRF's curves of the TDOF System with T_r = 4 s are shown in Figure 3, 4, and 5.

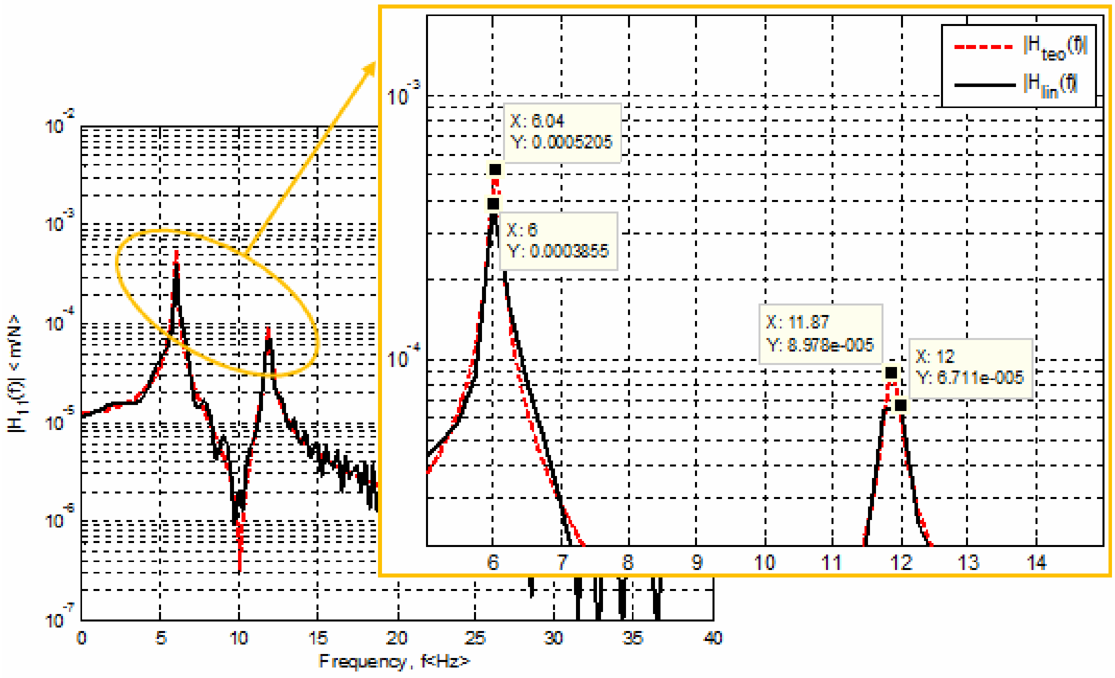

Figure 3. $H_{11}(f)$ of the TDOF System with T_r = 4 s.

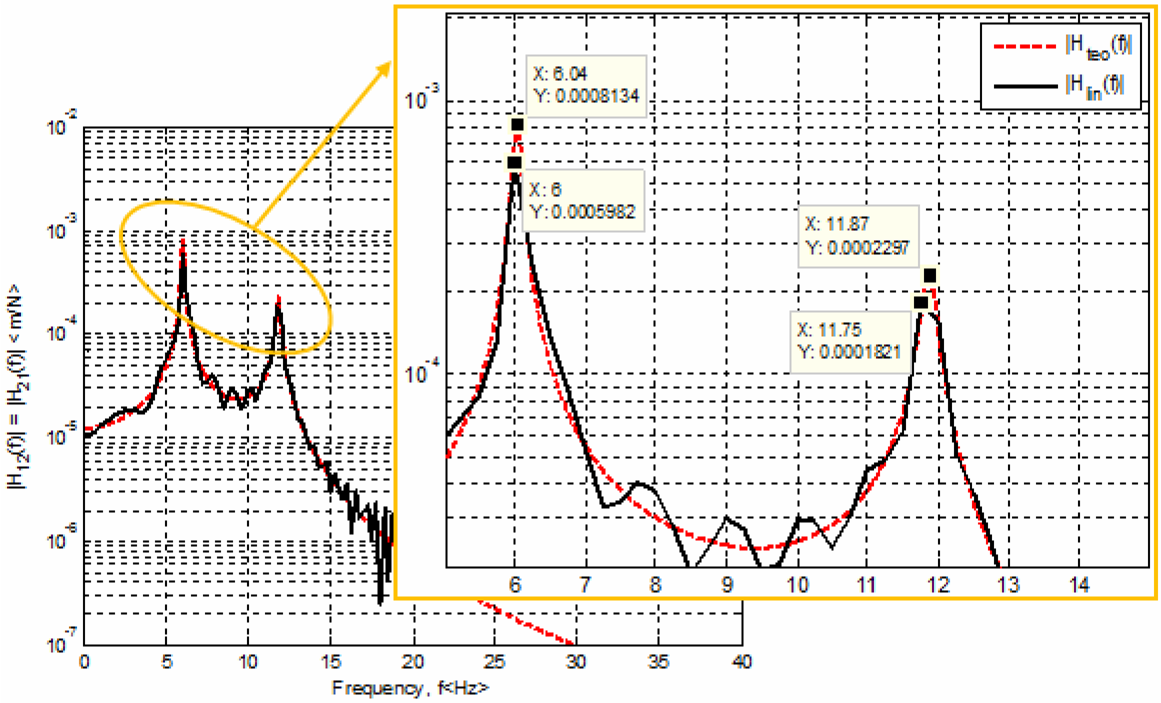

Figure 4. $H_{12}(f)$ or $H_{21}(f)$ of the TDOF System with T_r = 4 s.

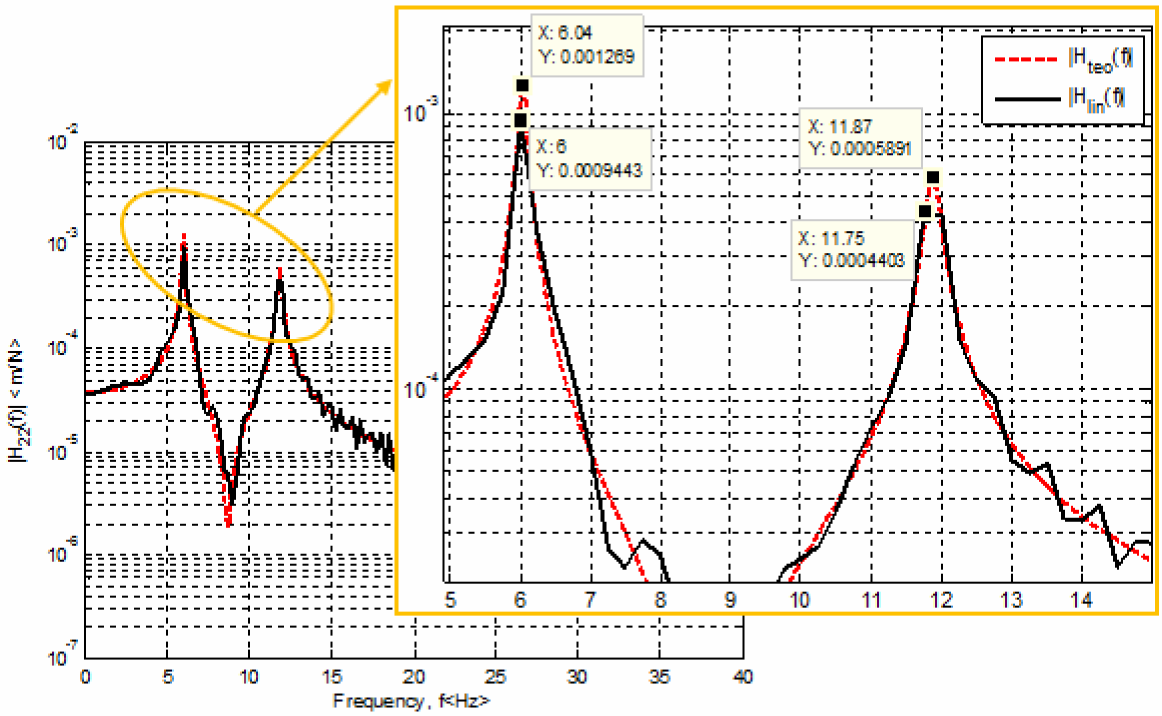

Figure 5. $H_{22}(f)$ of the TDOF System with T_r = 4 s.

The FRF's curves in Figure 3, 4, and 5 are shown the FRF's magnitude | $H_{ij}(f)$ | of the TDOF system. Accuracy of the FRF's curves established refers to error percentage of the obtained FRF's magnitude and resonant frequencies f_r values to its theoretical values at peak of the FRF's curves. The obtained FRF's magnitude using the linear swept-sine excitation and f_r values are compared to its theoretical values with 4 s, 8 s, and 16 s of T_r are shown in Table 2. The error percentage of the obtained FRF's magnitude and resonant frequencies f_r values to its theoretical values at peak of the FRF's curves are shown in Table 3.

Table 2. The obtained FRF's magnitudes using the linear swept-sine excitation and resonant frequencies values are compared to its theoretical values.

FRF	Theoretical			
	At the first peak of FRF's curve		At the second peak of FRF's curve	
	f_{r1} <Hz>	$\|H(f_{r1})\|$ <m/N>	f_{r2} <Hz>	$\|H(f_{r2})\|$ <m/N>
$H_{11}(f)$	6.04	52.05×10^{-5}	11.87	8.98×10^{-5}
$H_{12}(f)$ or $H_{21}(f)$	6.04	81.34×10^{-5}	11.87	22.97×10^{-5}
$H_{22}(f)$	6.04	126.90×10^{-5}	11.87	58.91×10^{-5}
FRF	Using the linear swept-sine excitation with $\boldsymbol{T_r}$ **= 4 s**			
	At the first peak of FRF's curve		At the second peak of FRF's curve	
	f_{r1} <Hz>	$\|H(f_{r1})\|$ <m/N>	f_{r2} <Hz>	$\|H(f_{r2})\|$ <m/N>
$H_{11}(f)$	6.00	38.55×10^{-5}	12.00	6.71×10^{-5}
$H_{12}(f)$ or $H_{21}(f)$	6.00	59.82×10^{-5}	11.75	18.21×10^{-5}
$H_{22}(f)$	6.00	94.43×10^{-5}	11.75	44.03×10^{-5}
FRF	Using the linear swept-sine excitation with $\boldsymbol{T_r}$ **= 8 s**			
	At the first peak of FRF's curve		At the second peak of FRF's curve	
	f_{r1} <Hz>	$\|H(f_{r1})\|$ <m/N>	f_{r2} <Hz>	$\|H(f_{r2})\|$ <m/N>
$H_{11}(f)$	6.00	45.32×10^{-5}	11.88	8.86×10^{-5}
$H_{12}(f)$ or $H_{21}(f)$	6.00	70.34×10^{-5}	11.88	22.50×10^{-5}
$H_{22}(f)$	6.00	111.00×10^{-5}	11.88	57.97×10^{-5}
FRF	Using the linear swept-sine excitation with $\boldsymbol{T_r}$ **= 16 s**			
	At the first peak of FRF's curve		At the second peak of FRF's curve	
	f_{r1} <Hz>	$\|H(f_{r1})\|$ <m/N>	f_{r2} <Hz>	$\|H(f_{r2})\|$ <m/N>
$H_{11}(f)$	6.06	47.40×10^{-5}	11.88	8.92×10^{-5}
$H_{12}(f)$ or $H_{21}(f)$	6.06	74.38×10^{-5}	11.88	22.74×10^{-5}
$H_{22}(f)$	6.06	115.30×10^{-5}	11.88	58.43×10^{-5}

Table 3. The error percentage of the obtained FRF's magnitude using the linear swept-sine excitation and resonant frequencies values to its theoretical values at peak of the FRF's curves.

FRF	Using the linear swept-sine excitation with $\boldsymbol{T_r}$ **= 4 s**			
	Error at the first peak of FRF's curve <%>		Error at the second peak of FRF's curve <%>	
	Error of f_{r1}	Error of $\|H(f_{r1})\|$	Error of f_{r2}	Error of $\|H(f_{r2})\|$
$H_{11}(f)$	0.66	25.94	1.10	25.28
$H_{12}(f)$ or $H_{21}(f)$	0.66	26.46	1.01	20.72
$H_{22}(f)$	0.66	25.59	1.01	25.26
FRF	Using the linear swept-sine excitation with $\boldsymbol{T_r}$ **= 8 s**			
	Error at the first peak of FRF's curve <%>		Error at the second peak of FRF's curve <%>	
	Error of f_{r1}	Error of $\|H(f_{r1})\|$	Error of f_{r2}	Error of $\|H(f_{r2})\|$
$H_{11}(f)$	0.66	12.93	0.08	1.34
$H_{12}(f)$ or $H_{21}(f)$	0.66	13.52	0.08	2.05
$H_{22}(f)$	0.66	12.53	0.08	1.60
FRF	Using the linear swept-sine excitation with $\boldsymbol{T_r}$ **= 16 s**			
	Error at the first peak of FRF's curve <%>		Error at the second peak of FRF's curve <%>	
	Error of f_{r1}	Error of $\|H(f_{r1})\|$	Error of f_{r2}	Error of $\|H(f_{r2})\|$
$H_{11}(f)$	0.33	8.93	0.08	0.67
$H_{12}(f)$ or $H_{21}(f)$	0.33	8.56	0.08	1.00
$H_{22}(f)$	0.33	9.14	0.08	0.81

The error of resonant frequency at peak of the FRF's curve of the obtained FRF using linear swept-sine excitation are less than 2 % for all T_r. In the meantime, the error of peak of the FRF's curve of the obtained FRF using linear swept-sine excitation are decrease with increase swept-time T_r.

CONCLUSION

This paper has been presented an analysis of accuracy of the FRF's curves obtained by using linear swept-sine excitation. From analysis has been done, it can be concluded that accuracy of the FRF's curves of the TDOF System depends on the duration of linear swept-sine excitation (swept time) of which applied to system. If swept-time of the linear swept-sine excitation applied to the TDOF System is increased, then error percentage of the obtained FRF's magnitudes and resonant frequencies of the TDOF System would be decrease.

REFERENCES

Baoliang, N. and Xia, Y. (2003): A FFT Based Variety Sampling Rate Sine Sweep Vibration Controller, *IEEE 2003 International Conference on Neural Networks & Signal Processing*, 2,1714 - 1718.

Climent, H. (2007): Aeroelastic and Structural Dynamics Tests at EADS CASA, *Proceeding of the 18th Annual Symposium of the Society of Flight Test Engineers SFTE*, Madrid.

Cloutier, D., Avitabile, P., Bono, R. and Peres, M. (2009): Shaker/Stringer Effect on Measured Frequency Response Functions, *27th International Modal Analysis Conference*, Florida.

Füllekrug, U., Böswald, M., Göge, D. and Govers, Y. (2008): Measurement of FRFs and Modal Identification in Case of Correlated Multi-Point Excitation, *Shock and Vibration*, 15(3), 435-445.

Gloth, G., and Sinapsis, M. (2004): Analysis of Swept-Sine Runs During Modal Identification, *Mechanical Systems and Signal Processing*, 18(6), 1421–1441.

Gloth, G., and Sinapius, M. (2004): Influence and Characterisation of Weak Non-Linearities in Swept-Sine Modal Testing, *Aerospace Science and Technology*, 8(2), 111-120.

Göge, D., Böswald, M., Füllekrug, U. and Lubrina, P. (2007): Ground Vibration Testing of Large Aircraft–State-of-the-Art and Future Perspectives, *25th International Modal Analysis Conference*, Florida.

Haritos, N. (2002): The Characteristics of Dynamic Systems via The Swept Sine Wave Technique, *Mathematics and Computers in Simulation*, 8(2), 111-120.

Kreyszig, E., (2006): *Advanced Engineering Mathematics 9th Edition*, John Wiley & Sons Inc., New York.

McConnell, K. G. (1995): *Vibration Testing: Theory and Practice*, John Wiley & Sons Inc., New York.

Mobley, R. K. (1999): *Vibration Fundamentals (Plant Engineering Maintenance (Hardback)*, Butterworth–Heinemann, Boston.

Ogata, K. (1995): *Discrete-Time Control Systems*, Prentice-Hall Inc., New Jersey.

Ogata, K. (2002): *Modern Control Engineering*, Prentice-Hall Inc., New Jersey.

Orlando, S., Peeters, B. and Coppotelli, G. (2008): Improved FRF estimators for MIMO Sine Sweep Data, *Proceedings of the ISMA 2008 International Conference on Noise and Vibration Engineering*, Leuven.

Pauwels, S., Michel, J., Robijns, M., Peeters, B. and Debille, J. (2006): A New MIMO Sine Testing Technique for Accelerated High Quality FRF Measurements, *24th International Modal Analysis Conference*, St. Louis.

Peeters, B., Hendricx, W. and Debille, J. (2008): Modern Solutions for Ground

Vibration Testing of Large Aircraft, *26th International Modal Analysis Conference*, Florida.

Peres, M. A., Bono, R. W. and Brown, D. L. (2010): Practical Aspects of Shaker Measurements for Modal Testing, *Proceeding of ISMA 2010*.

Scheffer, C. and Girdhar, P. (2004): *Machinery Vibration Analysis & Predictive Maintenance (Practical Machinery Vibration Analysis and Predictive Maintenance)*, IDC Technologies, Oxford.

Schwarz, B.J. and Richardson, M.H. (1999): *Experimental Modal Analysis*, in *CSI Reliability Week.*, Vibrant Technology Inc., Florida.

Yanto, A. and Abidin, Z. (2012): Developtment of Swept-sine Excitation Control Method to Minimize The FRF Measurement Error, *MEV (Mechatronics, Electrical Power, and Vehicular Technology) Journal*, 3, 57–64.

Yanto, A. and Abidin, Z. (2012): Numerical and Experimental Study of Swept-sine Excitation Control Method To Increase Accuracy of the FRF Measurement, *Proceeding of SNTTM and Thermofluid IV*, Yogyakarta, 2096-2101.

Yanto, A. (2013): Analysis Of Swept Time and Modal Parameter Effect On FRF's Magnitude Error Of SDOF System Using Linear Swept-Sine Excitation, *Momentum Journal*, 14(1), 18-24.

Zhuge, J. (2009): *Advanced Dynamic Signal Analysis*, Crystal Instruments Corp., Santa Clara.